The Spine Journal 19 (2019) 1871–1884

Basic Science

Biomechanical evaluation of calcium phosphate-based nanocomposite versus polymethylmethacrylate cement for percutaneous kyphoplasty

Qifeng Lu, PhD[a], Chun Liu, MS[a], Dingsong Wang, MS[b], Huiling Liu, MS[a], Huilin Yang, PhD[a], Lei Yang, PhD[a,*,1]

[a] *Orthopaedic Institute, Department of Orthopaedic Surgery, The First Affiliated Hospital of Soochow University, Suzhou, Jiangsu, China*

[b] *Department of Orthopaedics, Taizhou People's Hospital, Taizhou, Jiangsu, China*

Received 25 January 2019; revised 5 June 2019; accepted 6 June 2019

Abstract

BACKGROUND CONTEXT: Polymethylmethacrylate (PMMA) is the most commonly used filling material when performing percutaneous kyphoplasty (PKP) for the treatment of osteoporotic vertebral compression fractures. However, there are some inherent and unavoidable drawbacks with the clinical use of PMMA. PMMA bone cement tends to leak during injection, which can lead to injury of the spinal nerves and spinal cord. Moreover, the mechanical strength of PMMA-augmented vertebral bodies is extraordinary and this high level of mechanical strength might predispose to adjacent vertebral fractures. A novel biodegradable calcium phosphate-based nanocomposite (CPN) for PKP augmentation has recently been developed to potentially avoid these issues.

PURPOSE: By comparison with PMMA, the leakage characteristics, biomechanical properties, and dispersion of CPN were evaluated when used for PKP.

STUDY DESIGN: Biomechanical evaluation and studies on the dispersion and anti-leakage properties of CPN and PMMA cements were performed and compared using cadaveric vertebral fracture model, sheep vertebral fracture model, and simulated rigid foam model.

METHODS: Sheep vertebral bodies were decalcified by ethylenediaminetetraacetic acid disodium salt (EDTA-Na_2) to simulate osteoporosis *in vitro*. After compression to create wedge-shaped fractures using a self-designed fracture creation tool, human cadaveric vertebrae and decalcified sheep vertebrae were augmented by PKP. In addition, three L5 vertebral bodies from human cadavers were used in a contrast vertebroplasty (VP) augmentation experiment. Occurrence of cement leakage was observed and compared between CPN and PMMA during the process of vertebral augmentation. Open-cell rigid foam model (Sawbones#1522-507) was used to create a simulated leakage model for the evaluation of the leakage characteristics of CPN and PMMA with different viscosities. The augmentation effects of CPN and PMMA were evaluated in human cadaveric and decalcified sheep vertebral models and then compared to the results from solid rigid foam model (Sawbones#1522-23). The dispersion abilities of CPN and PMMA were evaluated via three methods as follows. The dispersion volume and dispersion ratio were calculated by three-dimensional reconstruction using human vertebral body CT scans; the ratio of cement area to injection volume was calculated from three-dimensional sections of micro-CT scans of a sheep vertebra; and the micro-CT images of cement dispersion in open-cell rigid foam model (Sawbones#1522-507) were compared between CPN and PMMA. This study was funded by the National Natural Science Foundation of China (No. 81622032, 190,000 dollars and No. 51672184, 90,600 dollars), Principal

FDA device/drug status: Not applicable.

Author disclosures: ***QL:*** Nothing to disclose. ***CL:*** Nothing to disclose. ***DW:*** Nothing to disclose. ***HL:*** Nothing to disclose. ***HY:*** Nothing to disclose. ***LY:*** Nothing to disclose.

* Corresponding author. Institute of Orthopaedics, The First Affiliated Hospital of Soochow University, No. 708 Renmin Road, Suzhou, Jiangsu 215006, China. Tel.: +86 512 6778 1540; fax: +86 512 6778 1165.

E-mail addresses: yleibrown@gmail.com, leiy@suda.edu.cn (L. Yang).

[1] Present address: Center for Health Science and Engineering, School of Materials Science and Engineering, Hebei University of Technology, Tianjin 300130, China.

https://doi.org/10.1016/j.spinee.2019.06.007

Project of Natural Science Research of Jiangsu Higher Education Institutions (No. 17KJA180011, 22,000 dollars), and Jiangsu Innovation and Entrepreneurship Program (146,000 dollars).

RESULTS: There was no significant difference in vertebral height between CPN and PMMA during PKP augmentation and both cements restored the vertebral height after augmentation. In PKP augmentation experiment, posterior wall cement leakage occurred in 75% of human vertebrae augmented with PMMA; however, no leakage occurred in human vertebrae augmented with CPN. Anterior leakage occurred in all vertebrae augmented by PMMA, while in only 75% of vertebra augmented by CPN. Furthermore, CPN and PMMA had completely different leakage patterns in the simulated rigid foam model whether administered at the same injection speed or under the same injection force, suggesting that CPN has anti-leakage characteristics. The augmentation in human cadaveric vertebrae was lower with CPN compared to PMMA (1,668±816 N vs. 2,212± 813 N, p=.459, respectively), but this difference was not significant. The augmentation force in sheep vertebral bodies reached 1,393±433 N when augmented with PMMA, but 1,108±284 N when augmented with CPN. The dispersion of CPN was better, and the dispersion volume and ratio were greater, with CPN than with PMMA. Imaging of the open-cell rigid foam model showed completely different dispersion modes for CPN and PMMA. After injection, the PMMA cement formed a contracted clump in the open-cell rigid foam model. However, the CPN cement extended many antennae outward, appearing to spread to the surrounding area. The surface areas of the CPN cement blocks with different liquid-to-solid ratios were significantly larger than the surface area of the PMMA cement in the open-cell rigid foam model ($p<.05$).

CONCLUSIONS: CPN has anti-leakage properties, which might be related to its high viscosity and viscoplasticity. CPN had a slightly lower augmentation force than PMMA when used in cadaveric vertebrae, decalcified sheep vertebrae, and in the standard rigid foam model. However, CPN diffused more easily into cancellous bone than did PMMA and encapsulated bone tissue during the dispersion process. The excellent dispersion of CPN generated better interdigitation with cancellous bone, which may be why the augmentation effect of CPN is similar to that of PMMA.

CLINICAL SIGNIFICANCE: Biodegradable CPN is a potential alternative to PMMA cement in PKP surgery, in which CPN is likely to reduce the cement leakage during the surgery and avoid the post-surgery complications caused by excessive strengths and nondegradability of PMMA cement.

Keywords: Calcium phosphate; Kyphoplasty; Osteoporosis; Polymethylmethacrylate; Vertebral compression fracture; Nanocomposite; Cement leakage; Biomechanics; Minimally invasive surgery

Introduction

Osteoporotic vertebral compression fracture (OVCF) is a common injury that can cause great pain and can impair quality of life in the elderly [1,2]. Vertebral augmentation by percutaneous kyphoplasty (PKP) has demonstrated efficacy for the treatment of (OVCF) [3]. Vertebral augmentation via PKP involves the injection of bone cement filling material into the vertebral body in an effort to rapidly relieve pain, stabilize the fractured vertebrae, and allow the patient to resume daily activities.

The most commonly used bone cement is polymethylmethacrylate (PMMA), however, some inherent and unavoidable drawbacks of PMMA have been reported. For example, there is 6.8%−21.9% probability that PMMA will leak during surgery [4,5]. Leakage of PMMA from the vertebral body can squeeze and burn spinal nerves and even the spinal cord due to its high polymerization temperature [6]. In addition, there is a 3.5%−28.6% chance that PMMA will leak into blood vessels and cause a pulmonary cement embolism [7]. Moreover, excessive physiological strength and the Young's modulus of PMMA can lead to adjacent vertebral fractures after augmentation [8]. In addition, PMMA is not biodegradable and remains in the body after injection, thus the monomer toxicity of PMMA can cause long-term damage [6].

A novel injectable calcium phosphate-based nanocomposite (CPN) was developed in a previous study done by our group [9−11]. CPN is a bone cement based on calcium phosphates and possesses good biodegradability and bone growth inductivity [9,10]. In standard *in vitro* degradability tests, CPN cement soaked in Tris-HCl had a weight loss of 6% after 7 days and 10.62% after 5 weeks [12]. In addition, the smooth outer surface of the cement had degraded and bone ingrowth was observed in femur defects in rats, *in vivo*, 8 weeks after CPN implantation [12]. Furthermore, gelatinized starch and calcium phosphate particles established a nanostructured network in CPN, resulting in enhanced mechanical properties than other calcium phosphate cements [11,12]. In a study of cement-injectable cannulated pedicle screws, CPN had similar biomechanical properties, including comparable pull-out force and torsion resistance, to PMMA, although the intrinsic mechanical strength of CPN was found to be only half that of PMMA [11,13]. The above results have been verified in simulated

osteoporotic bone models using decalcified sheep vertebrae and simulated rigid foam model [11,13].

Based on these results, the current study hypothesizes that CPN possesses appropriate mechanical augmentation strength to be used for PKP and that some of the drawbacks that occur with PMMA, such as leakage and adjacent vertebral fractures, will be lessened with the use of CPN. The purpose of this study was to evaluate the biomechanical properties and leakage characteristics of CPN for PKP application. The human cadaveric vertebral model, decalcified sheep vertebral model, and simulated rigid foam model, respectively were used to evaluate and compare the leakage characteristics, mechanical augmentation, and dispersion properties of CPN and traditional PMMA cement.

Materials and methods

Preparation of materials and specimens

Preparation of CPN

The chemicals used include alpha-tricalcium phosphate (Ensail Co., Ltd. Beijing, China), calcium hydrogen phosphate dehydrate ($CaHPO_4 \bullet 2H_2O$, DCPD, Sigma Aldrich, St. Louis, MO, USA), disodium hydrogen phosphate (Na_2HPO_4, Alfa-Aesar, Haverhill, MA, USA), barium sulfate ($BaSO_4$, BS, Sigma Aldrich, St. Louis, MO, USA), and food-grade pregelatinized starch (Jingrui New Material, Xuancheng, China). With the exception of the pregelatinized starch, all other chemicals were ball-milled overnight in ethanol for 15 hours at 1,400 rpm using a planetary ball mill (PM2L, DPLIFT Machinery Co., Ltd. Shanghai, China). After ball-milling, the slurry was dried at 80°C and ground into powder. For preparation of CPN [9], 20 wt.% BS and 20 wt.% pregelatinized starch were added to calcium phosphate cement, which was composed of alpha-tricalcium phosphate and DCPD at a mass ratio of 9:1. The setting liquid was a 0.25 mol/L Na_2HPO_4 solution and a liquid-to-solid ratio (L/S) of 0.4 mL/g was used for experiment. After mixing the cement powder with setting liquid, CPN became a semi-solid paste with high viscosity. This study formulated strict operating rules for the preparation of CPN cement, including the purchase of raw materials, the proportion of components in formulation, environment conditions, and the operational steps, so as to ensure the quality of CPN cement. Clinically used PMMA cement (Mendec Spine, Tecres SPA, Sommacampagna, Italy), at an L/S ratio of 0.5 mL/g, was used as the control for CPN. According to the previously reported method, the mechanical properties of bone cements were evaluated by uni-axial compression test [9,11]. Bone cement was molded into cylinders (6 mm in diameter and 12 mm in length) and the cylinders were compressed in a mechanical tester (HY-1080; Hengyi Group, Shanghai, China). The stress-strain curve was calculated and the mechanical strength was defined as maximum stress value in the curve. The compressive modulus was calculated using the linear range in the curve [9,11].

Human cadaver vertebrae

Three thoracolumbar spines, containing 24 vertebrae from T10 to L5, were harvested from elderly male cadavers, aged from 72 to 86 years. This study was approved by the Human Research Ethics Committee of Taizhou People's Hospital (No. KY201809301), complying with China's relevant laws and regulations. Bone mineral density (BMD) of the harvested spines was measured using dual energy radiograph absorptiometry (XR-800, Norland, New Jersey, USA) and was found to be 2.5 standard deviations below the young adult mean, thus meeting the diagnostic criteria for osteoporosis [14].

Preparation of decalcified sheep vertebrae for osteoporosis simulation

Due to legal and ethical constraints, the number of cadaveric vertebral specimens was limited in this study. Therefore, decalcified sheep vertebral bodies were used to carry out more detailed evaluations, so that the results of cadaveric and sheep vertebral specimens could be mutually verified, thus ensuring the reliability of the experimental results. Fresh lumbar 1–4 vertebral bodies from 1.5-year-old sheep (weighing 50–60 kg) were purchased from a slaughterhouse for all experiments. All appendages were removed from the sheep lumbar vertebrae. Only the pedicle and vertebral body were preserved. The vertebral body was immersed in 20% ethylenediaminetetraacetic acid disodium salt solution at room temperature for 10 days, thus achieving decalcification to simulate osteoporosis.

Rigid foam model

Commercially available open cell rigid foam model (Sawbones#1522-507, Pacific Research Laboratories, Inc, Vashon, WA, USA) was the osteoporotic simulated testing material used in this study. This open rigid foam model has a density of 0.12 g/cm^3 and a 95% open-celled porous structure similar to that of human cancellous bone with severe osteoporosis, thus providing a uniform standard testing material [15]. A different rigid foam model, a solid rigid foam (Sawbones# 1522-23; Pacific Research Laboratories, Inc., Vashon, WA, USA), was the biomechanical testing material utilized in this study. This solid rigid foam model has a close cell content and a density of 0.08 g/cm^3 in accordance with the ASTM F-1839-08 standard and has the same mechanical properties as cancellous bone for the mechanical compression test [15].

Surgical techniques

Vertebral fracture model

The same method was used to produce fracture models in both the human cadaver vertebrae (21 vertebrae from

T10 to L4) and the sheep vertebrae. The upper and lower ends of all vertebral bodies were embedded with tooth powder (Boer Chemical Co., Ltd., Shanghai, China) and polished to keep them parallel. After that, five evenly distributed pores [16,17] (1.5 mm in diameter, and 2 mm in depth) were drilled in the upper one-fourth anterior area of each vertebra. A self-designed fracture creation tool was used to create wedge-shaped fractures in the mechanical tester (HY-1080; Hengyi Group, Shanghai, China; Supplementary Fig. S1a). Vertical loading was carried out at a loading rate of 2 mm/min until the height of the front edge of the vertebral body was reduced by 25% [18,19] (Supplementary Fig. S1a). The force-displacement curve and related data were recorded. The initial fracture strength (IFS) of each vertebral body was defined as the first peak load of the force-displacement curve [18,19].

PKP augmentation experiment

Human cadaver vertebrae: A total of 16 fractured vertebral bodies were selected from T10 to L4 vertebrae and paired to form eight groups (n=2/group), in which BMD, IFS, and vertebral size were relatively close. The PKP augmentation operation was simultaneously performed on the two vertebrae in each group. The inflatable bone tamp (IBT; Weigao Orthopaedic Device, Weihai, China) was inserted through the bilateral pedicle under X-ray monitoring (Radiation 60 kV and 2.5 mAs; SPL-HF-VET-4.0, SEDECAL, Spain). The bilateral tamp dilated simultaneously, at the same speed, and the filling volume of each tamp was equal in the paired group (Supplementary Fig. S1b). After the vertebral height was restored, the injection of bone cement was carried out at 21°C. After waiting for the doughing period (CPN) or drawing period (PMMA), PMMA or CPN cement was injected at 22% of the average volume of each vertebral body. The injection was performed on a mechanical tester at an injection speed of 300 mm/min.

Decalcified sheep vertebrae: The PKP instruments used for the decalcified sheep vertebrae were the same as those used for the human cadaver vertebrae. However, unilateral PKP augmentation was performed in the sheep vertebrae. After the vertebral height was restored by IBT, all vertebral bodies were randomly assigned to either a CPN or a PMMA group. Cement injection was performed on a mechanical tester at an injection speed of 300 mm/min. If the cement flowed out of the vertebral body, the injection was immediately stopped.

Contrast vertebroplasty (VP) augmentation experiment for human cadaveric vertebrae

In order to avoid individual differences between vertebral bodies, contrast VP augmentation experiment was designed for this study, in which different bone cements were injected into the same vertebral body in order to perform comparative tests. Three L5 vertebral bodies from human cadavers were used for the VP augmentation experiment. Under fluoroscopic guidance, an 11-gauge cannula (Weigao Orthopaedic Device) was inserted through the bilateral pedicle (Supplementary Fig. S1c). One side of the vertebral body was randomly assigned, according to computer-generated random numbers, to be injected with CPN; the other side was injected with PMMA as a control. Then 1.4 mL of CPN was injected into one side and 1.4 mL PMMA was injected into the other side of the same L5 vertebral body. The bone cement was injected at a speed of 300 mm/min using a mechanical tester, as above. The displacement-force curves of CPN and PMMA were recorded during the cement injection and the maximum peak value of the mechanical curve was defined as the injection force of cement.

Cement leakage evaluation

Leakage evaluation in cadaveric vertebrae

The cement leakage in the anterior and posterior wall of the vertebral body was compared between CPN and PMMA in the PKP augmentation experiment. First, the researchers observed and recorded the cement leakage sites in the anterior and posterior wall with the naked eye after the injection of bone cement, and then calculated average number of leakage sites (ANLS; ANLS=number of leakage sites/number of vertebrae). CT (Brightspeed CT/e, GE Healthcare, Chicago, IL, USA) was used to scan the augmented vertebral body to observe and confirm the occurrence of leakage (Fig. 1a, b).

All cement leakage was recorded and compared in the VP augmentation experiment. The method used was the same as the one discribed above. Leakage was observed with the naked eye and CT as used to evaluate the cement leakage in three augmented L5 vertebral bodies (Fig. 1c, d).

Leakage evaluation in the simulated leakage model

Based on the previous studies of leakage models produced using open cell porous materials [20,21], an open cell rigid foam model (Sawbones#1522-507) was used as the osteoporotic simulated material (40 mm×40 mm×60 mm) to establish a simulated leakage model in the current study. A 5 mm diameter perforated channel was produced in the middle and lower part of the open cell rigid foam model. Establishment of the channel was used to simulate the vessels in vertebral body. The open cell rigid foam model was then immersed in molten lard and vacuumed for 2 hours at 60°C. The lard was then allowed to solidify at room temperature, so as to simulate bone marrow in cancellous bone. During the testing process, a standard cement injector (Weigao Orthopaedic Device) was inserted into the middle of the simulated leakage model, just above the channel, and the top of injector was 5 mm away from the channel wall (Fig. 2a). Equal volumes of bone cement (1.4 mL), [including CPN in doughing period, PMMA in drawing period, and PMMA with high viscosity (the viscosity was increased to the level of CPN, Supplementary Fig. S2a–c)], were injected into the simulated leakage model at a speed of 300 mm/min and under a fixed injection force of

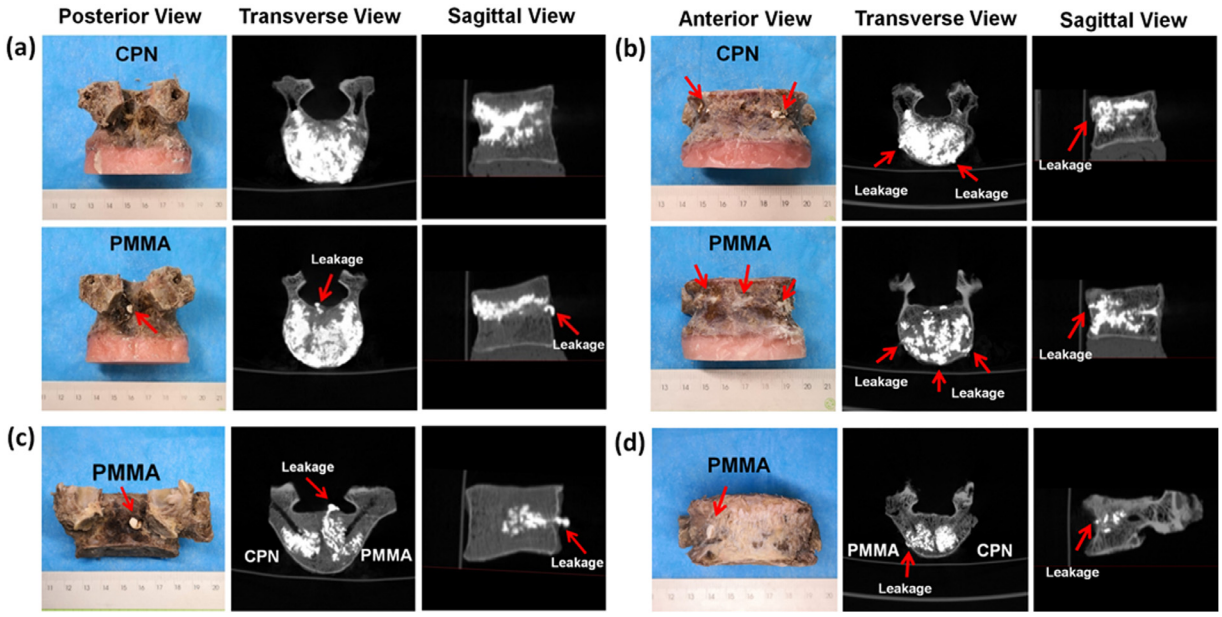

Fig. 1. Bone cement leakage in PKP augmentation and contrast VP augmentation experiments for human cadaveric vertebrae. (a,b) Typical photos and CT images of bone cement leakage during PKP augmentation: leakage from (a) posterior wall and (b) anterior wall. (c,d) Typical photos and CT imaging of augmented vertebral body in VP augmentation experiments showing the cement leakage from (c) posterior wall and (d) anterior wall. (Red arrow indicates the leakage sites).

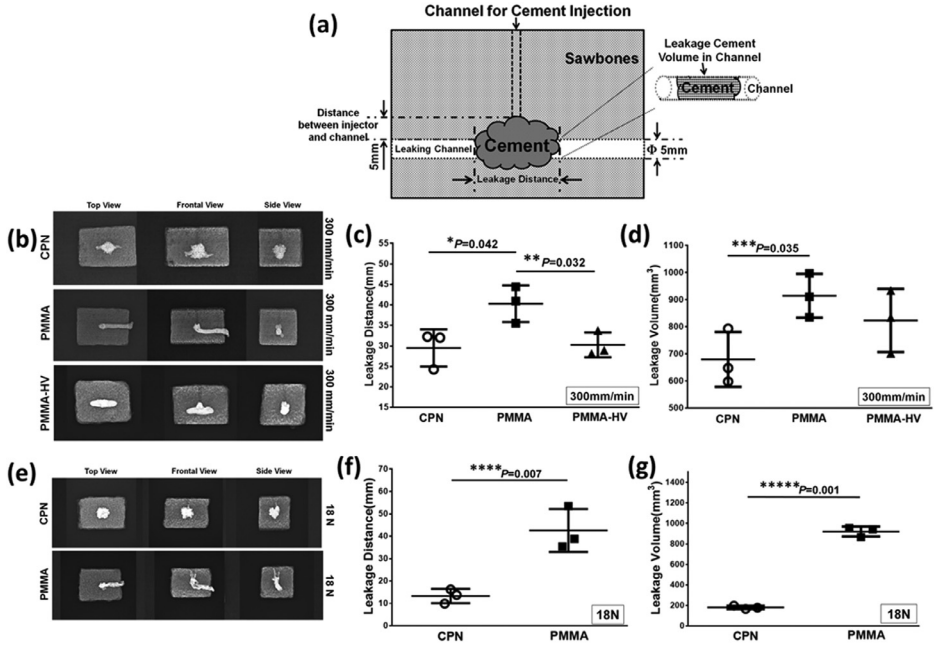

Fig. 2. Bone cement leakage in simulated leakage model: (a) schematic showing the preparation of the simulated leakage model; (b) typical X-ray images of bone cement leakage for CPN, PMMA (drawing period), and PMMA-high viscosity (HV) (the viscosity of PMMA was increased to the level of CPN) at 300 mm/min injection speed; (c) comparison of leakage distance between CPN, PMMA (drawing period) and PMMA-HV at 300 mm/min injection speed (*p=.042, **p=.032); (d) comparison of leakage volume between CPN, PMMA (drawing period) and PMMA-HV at 300 mm/min injection speed (***p=.035); (e) typical X-ray images of bone cement leakage for CPN and PMMA (drawing period) under the injection force of 18 N; (f) comparison of leakage distance between CPN and PMMA (drawing period) under the injection force of 18 N (****p=.007); (g) comparison of leakage volume between CPN and PMMA (drawing period) under the injection force of 18 N (*****p=.001).

18 N. In order to evaluate the extravasation tendency, the leakage distance in the channel was measured via radiographic X-ray film and the cement leakage volume in the channel was calculated by micro-CT (Skyscan 1176, Bruker micro-CT). When injected at 300 mm/min, the displacement-force curves of CPN and PMMA were recorded and the maximum peak value of curves was defined as injection force.

Evaluation of augmentation effects of bone cement

Augmentation effects for PKP augmented vertebrae

All augmented cadaveric vertebrae and sheep vertebrae were evaluted by compression test using the fracture creation tool on the mechanical tester, according to the previously described fracture model creation protocol (Fig. 3a). Augmentation strength was defined as the maximum compressive force recorded up to the deformation at IFS in the vertebral fracture model [22] (Fig. 3a).

Mechanical compressive test for VP augmented cadaveric vertebrae

After injection of bone cement, the augmented cancellous bones were removed and made into bone blocks of cylindrical shapes (Fig. 4a). Standard compression test for bone blocks was then performed on a mechanical tester. For the standard mechanical compression test, the value for stress was reported instead of force in order to eliminate the deviation caused by different sizes of the test samples. Thus, the compressive stress of cancellous bones was defined as the peak value of the first compression stress-strain curve.

Evaluation of augmentation effects by the solid rigid foam model

Based on the previous method using cement rigid foam model [23], a solid rigid foam model (Sawbones®#1522-23) was used to evaluate the augmentation effect of bone cement. After cutting, this biomechanical test material was fashioned into the shape of a cylinder, 30 mm in diameter and 19.8 mm in height. The shape and size of the model was similar to that of T6–T8 thoracic vertebral bodies [24–26].

The cylinder was then cut in half and rotated out of two 16-mm-diameter hemispherical cavities. When the two hemispheric cavities were glued together, a spherical cavity about 16% of the total volume was formed in the cylinder, simulating the cavity dilated by IBT in the compressed vertebral body (Fig. 5a). PMMA or CPN cement was then injected into the cavity, which simulated the PKP cement augmentation. In the standard mechanical compressive test, the 2 mm/min loading rate was used to uniaxially compress the augmented rigid foams on a mechanical tester and stress-strain curves were recorded. The compressive strength was determined by the first peak stress from the curve.

Evaluation of bone cement dispersion

CT scan for augmented cadaveric vertebrae

Three-dimensional CT-scan reconstruction was performed on the augmented human cadaver vertebrae in order to calculate the dispersion volume of the bone cement in the vertebrae and to obtain the dispersion ratio (dispersion volume/injection volume). The differences in dispersion between CPN and PMMA were then compared (Fig. 6a).

Micro-CT scan for augmented sheep vertebrae

The augmented sheep vertebral bodies were scanned via micro-CT and cross-sectional images of dispersed bone cement were obtained from the horizontal, coronal, and

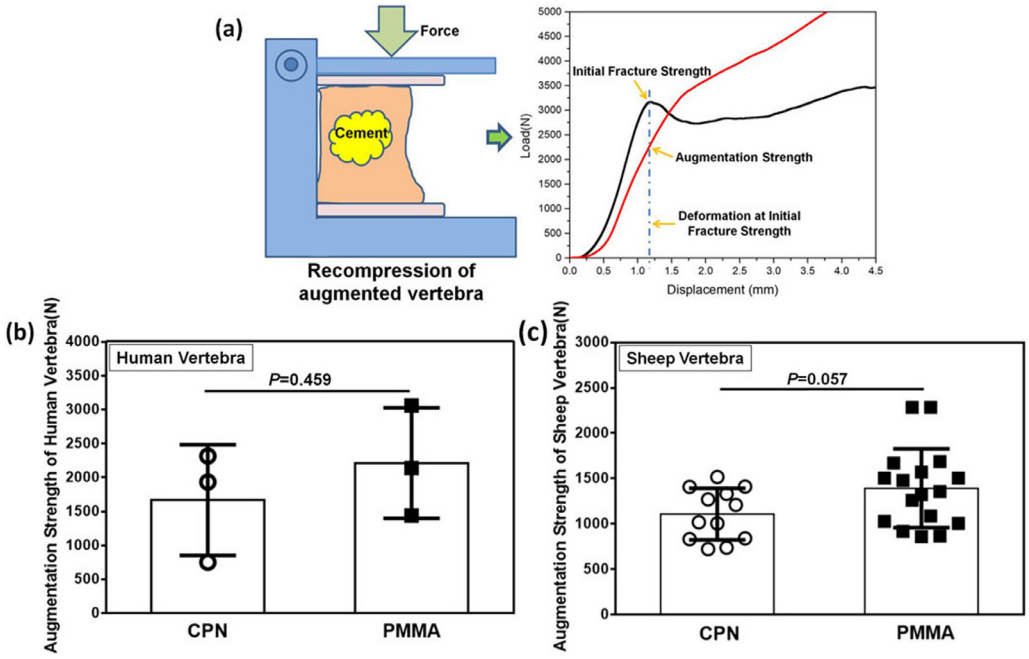

Fig. 3. Mechanical evaluation of bone cement augmentation in PKP experiments in human cadaveric vertebrae and decalcified sheep vertebrae: (a) schematic showing recompression of augmented vertebra and definition of augmentation strength; (b) comparison results of augmentation strength between CPN and PMMA cement for human cadaveric vertebral body (p=.459); (c) comparison for augmentation strength for decalcified sheep vertebral body (p=.057).

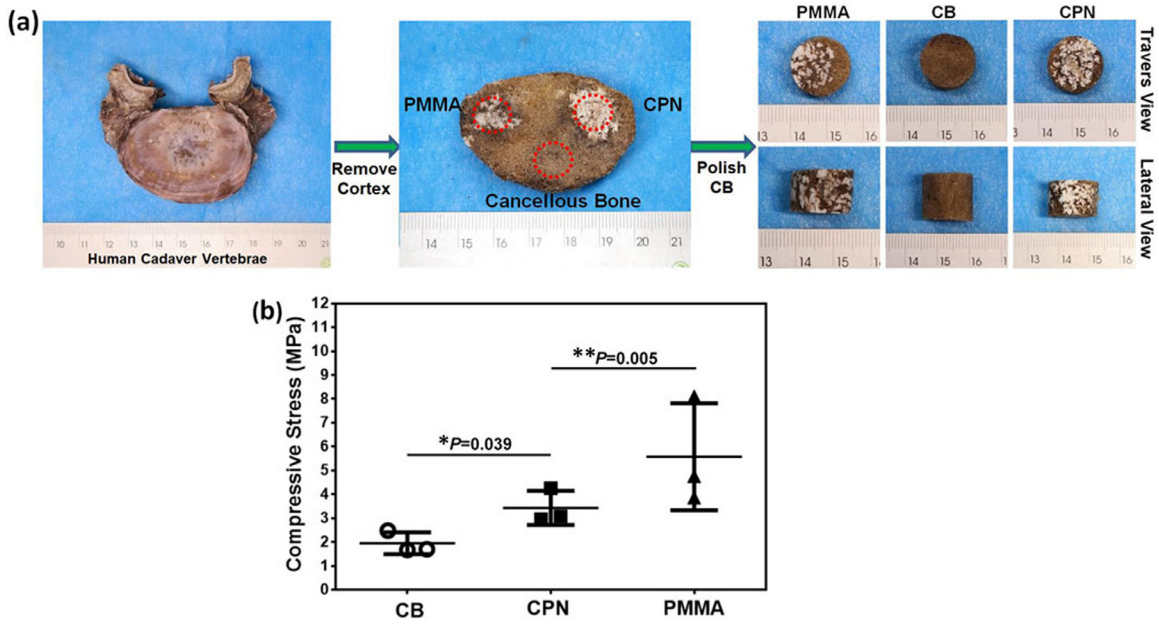

Fig. 4. Cancellous bone augmentation in human cadaveric vertebrae as shown by contrast VP experiment: (a) photo showing the extraction and polishing process of augmented cancellous bone in preparation for the compression test; (b) compressive stress of cancellous bones augmented by CPN and PMMA. (*p=.039, **p=.005). CB, cancellous bones.

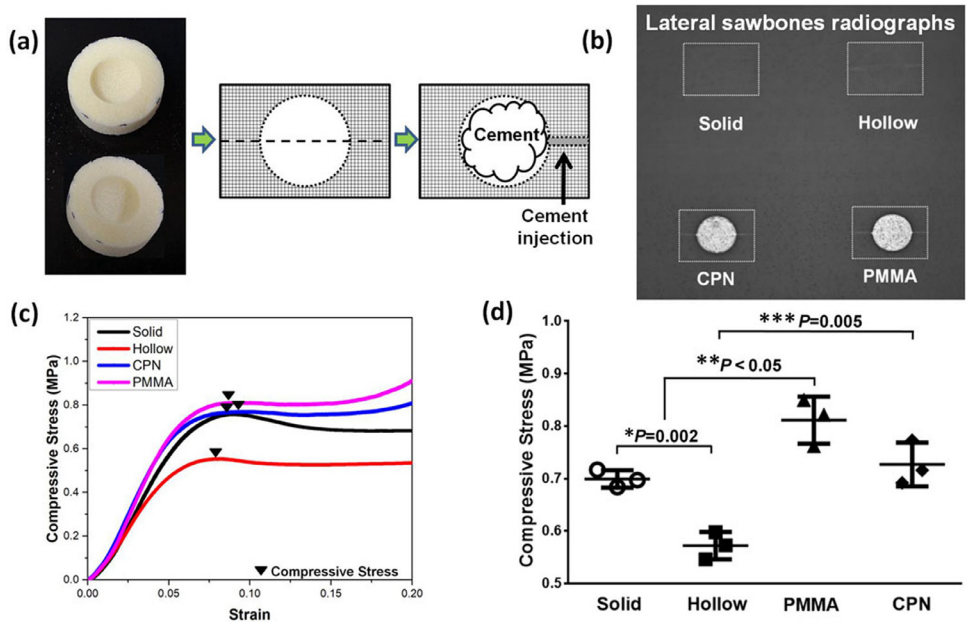

Fig. 5. Augmentation effects of bone cement in the solid rigid foam model: (a) photo and schematic showing the cement injection process in the solid rigid foam model (D=30 mm, H=19.8 mm) with a spherical cavity (D=16 mm); (b) radiographs of the solid rigid foam model injected with bone cement; (c) representative compressive stress-strain curve of solid rigid foam model injected with CPN or PMMA; (d) comparison results of compressive strength: solid versus hollow (*p=.002), PMMA versus controls (solid and hollow) (**p<.05), CPN versus hollow (***p=.005).

sagittal planes (Fig. 7a). Twenty-one uniformly distributed cross-sectional bone cement images were then taken from each plane for cement dispersion analysis. The cement areas of each cross-section were calculated and then divided by injection volumes and the ratio of the area to volume was used to compare the dispersion between CPN and PMMA.

Bone cement dispersion in open cell rigid foam model

An open-cell rigid foam model (Sawbones#1522-507) was used in this study to imitate osteoporotic bone. CPN (1.4 mL) with different L/S ratios (0.4, 0.6, 0.8, and 1.0) and PMMA cement of the same volume were injected into the open-cell rigid foam model (40 mm×

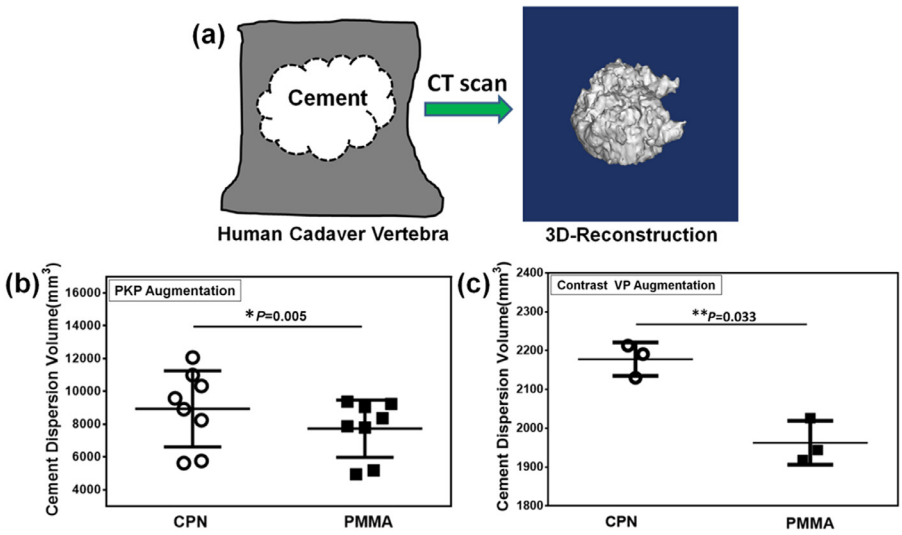

Fig. 6. Bone cement dispersion in human cadaveric vertebrae after PKP augmentation and contrast VP augmentation: (a) schematic showing three-dimensional reconstruction of CT scan for augmented vertebral body that was used to calculate dispersion volume; (b) comparison of dispersion volume between CPN and PMMA in PKP augmentation experiment (*p=.005); (c) comparison dispersion volume between CPN and PMMA in contrast VP augmentation experiment (**p=.033).

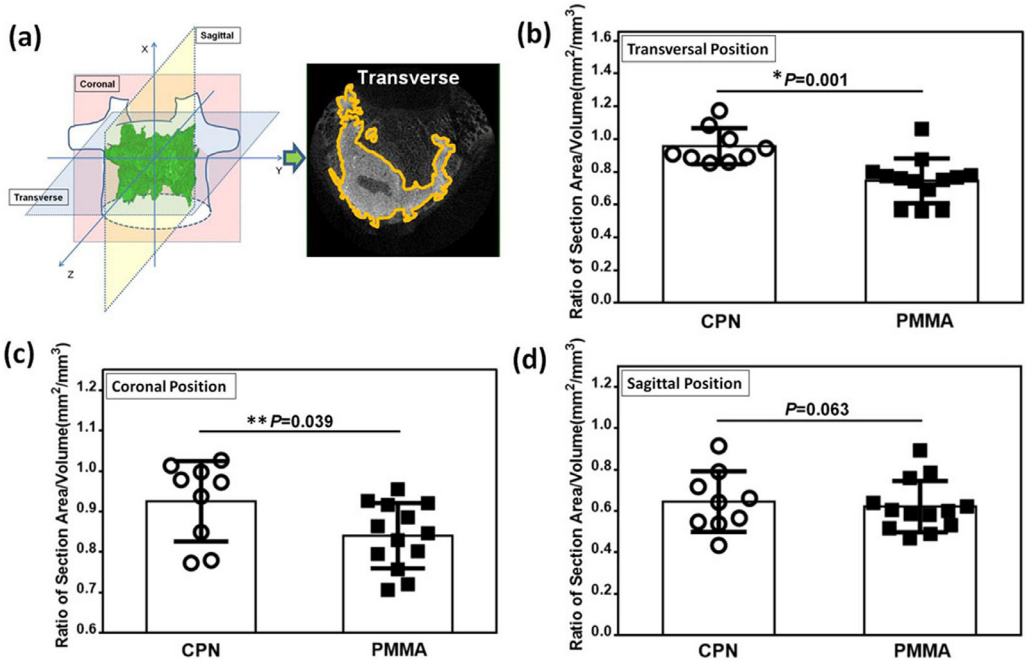

Fig. 7. PKP augmentation using PMMA and CPN cement in decalcified sheep vertebrae: (a) schematic and micro-CT imaging revealing the methods for obtaining the cement cross-section and area calculation for cement dispersion analysis; (b) ratio of cement transverse section area to volume (*p=.001), (c) ratio of cement coronal section area to volume (**p=.039); (d) ratio of cement sagittal section area to volume (no significant difference, p=.063).

40 mm×40 mm) using a standard injector connected to a mechanical tester at an injection speed of 300 mm/min. The displacement-force curves were recorded and the maximum peak value was determined as the injection force of cement. After cement injection, the open-cell rigid foam model was scanned via micro-CT and the surface area of the cement was calculated and compared between CPN and PMMA (Fig. 8).

Statistical analysis

The data in this study were processed by IBM SPSS Statistics 19.0 (SPSS Inc, Chicago, IL, USA), Origin 9.2 (OriginLab, Northampton, MA, USA), and GraphPad Prism 6 (GraphPad Software Inc, San Diego, CA, USA). For comparison of data between different groups, an independent or paired sample *t* test was used for continuous variables, and

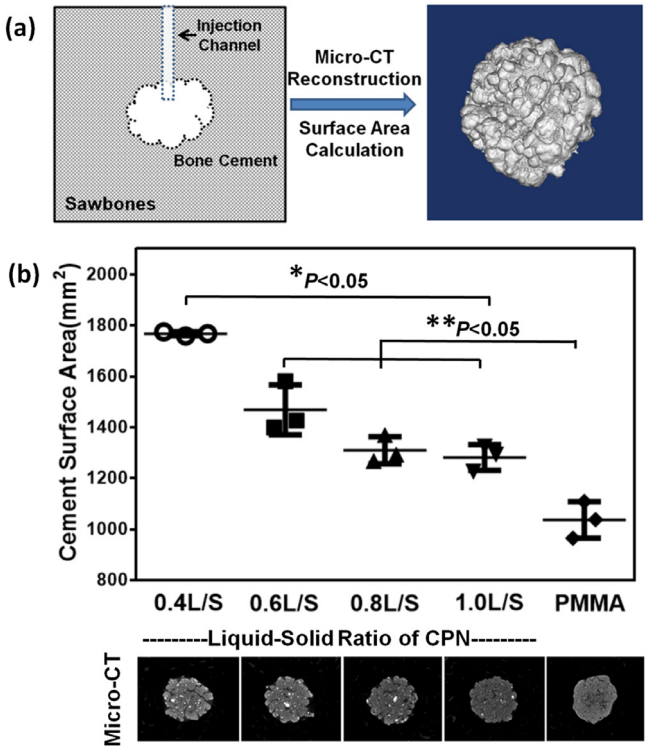

Fig. 8. Bone cement dispersion in the open-cell rigid foam model: (a) schematic revealing the calculation of surface area through micro-CT reconstruction; (b) comparison of surface area between PMMA and CPN with different liquid-to-solid ratios: 0.4 L/S-CPN versus other cement (*p<.05), PMMA versus other CPN cement (**p<.05).

a Chi squared or Fisher's exact test was used for categorical variables. A p value of less than .05 was considered to be statistically significant.

Results

Osteoporosis simulation of sheep vertebrae

The porous structure of the bone trabecula gradually eroded with the prolongation of decalcification time. The porous trabecular structure was destroyed and intersected with the surrounding voids, increasing the cell space of the trabecular bone. Bone mineral density also gradually decreased gradually as decalcification time increased (Supplementary Fig. S3a). After decalcifying for 10 days, the BMD of sheep vertebrae decreased from 0.60±0.06 g/cm^2 to 0.40±0.05 g/cm^2, or 65.98% of the original BMD (p<.05, Supplementary Fig. S3b). The mechanical curves indicated high repeatability (Supplementary Fig. S3c, d). The average IFS of the decalcified sheep vertebrae was 2,845±408 N (2,388 N−3,644 N), which was significantly lower than that of fresh vertebrae (4,985±726 N; p<.05, Supplementary Fig. S3e).

Vertebral compression fracture model for human cadaver vertebrae

A vertebrae compression fracture model, with high repeatability, was successfully established using human cadaver vertebrae. After compessing the vertebrae using the fracture creation tool, the height of the anterior vertebral body decreased to about three-fourths of the original height; however, the posterior wall of the vertebral body was basically intact with only about a 2 mm reduction during in the process of compressing the vertebrae (Supplementary Fig. S1a, Table. 1). Furthermore, pre-damaged pores ensured that the fracture lines all occurred in the upper part of the vertebral body (Supplementary Fig. S1a). Thus, the common wedge-shaped compression fracture was created, which is in accordance with the type A1.2 fracture [27] seen clinically. The PKP augmentation operation was successfully performed in the vertebral fracture model (Supplementary Fig. S1b). The height of fractured vertebrae was well restored after augmentation in both the PMMA and CPN groups. In the CPN group, the fractured anterior vertebral height was restored from 18.4±2.1 mm to 23.3±3.1 mm after augmentation (p=.002). In PMMA group, the anterior vertebral height recovered significantly from 18.2±1.4 mm to 23.8±1.8 mm (p=.000, Table. 1).

Injection force of bone cement

The injection force of CPN (38.8±8.4 N) was higher to that of PMMA (17.9±3.9 N, p=.015) based on the results of the contrast VP augmentation experiment (Supplementary Fig. S4a). Moreover, when bone cement was injected into the open-cell rigid foam model (Sawbones#1522-507), the injection force was higher with the 0.4 L/S ratio CPN compared to CPN with other L/S ratios (0.6, 0.8, and 1.0; p<.05). The average injection force of PMMA was 13.6±2.0 N, which was significantly lower than that of CPN with a 0.4 L/S ratio (32.8±5.5 N, p=.001; Supplementary Fig. S4b). These test results indicate that, although the injection force of 0.4 L/S CPN used in the experiment was about 20 N higher than that of PMMA (Supplementary Fig. S4a, b), the injection force of CPN was still within a reasonable range for clinical use (usually <50 N).

Evaluation of bone cement leakage

PKP and VP augmentation experiments in cadaveric vertebrae

For PKP augmentation experiment, as shown in Table 2, six vertebral bodies augmented by PMMA had posterior wall leakage (75%) in the eight paired groups, while no posterior wall leakage occurred in all the eight vertebra augmented by CPN (Fig. 1a and Table 2). The average number of posterior leakage sites in PMMA group was 1 per leaked vertebra (Table 2). Due to the severe anterior wall ruptures when creating the vertebral fracture model, both CPN and PMMA groups had a higher probability of anterior wall leakage than posterior wall leakage (Fig. 1b). However, the anterior leakage occurred in all vertebra augmented by PMMA while in only 75% of vertebra augmented by CPN (Table 2). Moreover, the average number of anterior leakage sites in PMMA group was 2.8 per leaked

Table 1
Height change and restoration in human cadaveric vertebral body after PKP

	Anterior height (mm)			Posterior height (mm)		
Group	Initial	After fracture†	After PKP‡	Initial	After fracture	After PKP
CPN	25.0±3.1	18.4±2.1	23.3±3.1	26.9±2.5	25.1±2.3	25.8±2.7
PMMA	25.1±2.2	18.2±1.4	23.8±1.8	27.0±2.9	25.5±2.9	26.0±3.2
p value*	.962	.828	.730	.932	.759	.879
	Midline height (mm)					
	Left side (mm)			Right side (mm)		
Group	Initial	After fracture†	After PKP‡	Initial	After fracture†	After PKP
CPN	25.3±2.7	21.5±2.2	24.6±2.3	25.2±2.3	21.9±2.5	24.7±2.6
PMMA	25.7±2.6	22.2±1.9	24.8±2.4	25.4±2.4	22.2±2.1	24.4±2.3
p value*	.813	.520	.892	.869	.781	.838

* Independent sample *t* test between CPN and PMMA groups.
† Versus initial height, independent sample *t* test, p<.05.
‡ Versus fractured height independent sample *t* test, p<.05.

Table 2
Cement leakage from posterior and anterior wall during the PKP augmentation of human cadaveric vertebra

Cement	CPN	PMMA
	Posterior wall leakage	
# of leaked vertebra	0 of 8 tested (0%)	6 of 8 tested (75%)
ANLS per leaked vertebra	0	1
	Anterior wall leakage	
# of leaked vertebra	6 of 8 tested (75%)	8 of 8 tested (100%)
ANLS per leaked vertebra	2.2	2.8

ANLS, average number of leakage sites.

vertebra, significantly higher than that in CPN group (Table 2).

In VP augmentation experiment, after three L5 vertebral bodies were injected with bone cement, the PMMA injection side of two vertebrae showed leakage out of the anterior or posterior wall of the vertebral body (66.7%), but no leakage occurred on the CPN injection side (Fig. 1c, d; Supplementary Fig. S5a, b).

Leakage evaluation in simulated leakage model

CPN and PMMA had completely different leakage patterns in the simulated leakage model even when administered at the same injection speed or under the same injection force. As shown by X-ray images, at an injection speed of 300 mm/min, the majority of the PMMA cement (injected during its drawing period) flowed along the channel in only one direction; however, the penetrating channel had little effect on CPN, which dispersed evenly. Only a small amount of CPN cement flowed uniformly to both ends of the channel (Fig. 2b). The leakage distance of PMMA was obviously greater than that of CPN (p=.042; Fig. 2c). Furthermore, the leakage volume of PMMA was also much greater than that of CPN (p=.035; Fig. 2d). When the viscosity of PMMA was increased to the level of CPN, the leakage distance and volume of PMMA were both reduced (Fig. 2c, d), but the PMMA leakage pattern was still different from that of CPN (Fig. 2b). Most of the high viscosity PMMA was blocked in the channel, however PMMA leakage distance and volume were still greater compared to CPN (Fig. 2c, d). In addition, PMMA with the same viscosity as CPN was close to the final hardening stage (Supplementary Fig. S2b, c), and the required injection force for PMMA (60.1±4.4 N) was nearly twice that of CPN (31.1±1.2 N) (Supplementary Fig. S2d), making it difficult to inject manually. The excessive injection force makes the high viscosity PMMA clinically impractical for PKP application.

As shown in Fig. 2e, the tendency for unidirectional leakage with PMMA (injected during the drawing period) is more obvious under an injection force of 18 N, while CPN diffused evenly and there was no obvious leakage at 18 N. The leakage distance was obviously greater with PMMA than with CPN (p=.007; Fig. 2f). Similarly, leakage volume was significantly larger with PMMA than with CPN (p=.001; Fig. 2g). In addition, high viscosity PMMA could not be expelled from the cement injector with an injection force of 18 N and thus could not be tested in the simulated leakage model.

Augmentation strength of bone cement

PKP experiment in human cadaveric vertebrae and sheep vertebrae

The strength of human cadaveric vertebrae after CPN augmentation was 1,668±816 N, which was lower than that after PMMA augmentation (2,212±813 N), however, this difference was not significant (p=.459; Fig. 3b). A similar result was observed in sheep vertebrae. The strength of sheep vertebral bodies augmented by PMMA reached 1,393±433 N, while that of sheep vertebral bodies augmented by CPN was 1,108±284 N. However, the difference between CPN and PMMA for the augmentation strength of sheep vertebrae was not significant (p=.057; Fig. 3c).

Table 3
Mechanical strength and moduli of bone cements

Cement	Compressive strength (MPa)	Modulus (GPa)
CPC	13.45±2.86	0.46±0.13
CPN	51.27±5.3	1.08±0.37
PMMA	93.48±11.27	1.87±0.23

Note: Data presented as mean ± standard deviation.
CPC, calcium phosphate cement; CPN, calcium phosphate nanocomposite; PMMA, polymethylmethacrylate.

Contrast VP augmentation experiment in human cadaveric vertebrae

The mechanical compressive test results for augmented cancellous bone suggest that both PMMA and CPN cement significantly enhanced the compressive strength of cancellous bone (p<.05; Fig. 4b). PMMA cement increased the compressive strength by about 250%, from 1.95 to 5.24 MPa. Moreover, the compressive strength of the cancellous bone augmented by CPN was 3.43 MPa, which was increased by 175%. The compressive strength of the cancellous bone augmented by CPN reached 65% of that augmented by PMMA. This ratio (65.46%) exceeded the ratio of intrinsic compressive strength for CPN/PMMA, which is only 55% (Table 3). This increase in the ratio of compressive strength indicates that CPN had a better augmentation effect on cancellous bone compared to PMMA.

Augmentation effects in the solid rigid foam model

Radiographs of the solid rigid foam model showed that the spherical cavity was fully filled with bone cement (Fig. 5b). The stress-strain curves of CPN and PMMA (Fig. 5c) indicate that compressive strength was significantly higher for both PMMA and CPN compared to the hollow rigid foam model with no cement filling (p<.05). The compressive strength of the rigid foam model augmented by CPN was just slightly lower than that of the rigid foam model injected with PMMA (0.727±0.042 MPa vs. 0.811±0.045 MPa, respectively), and the difference was not significant (p=.076).

Bone cement dispersion

Bone cement dispersion in human cadaveric vertebrae

In the PKP augmentation experiment, the dispersion volume of CPN was significantly higher than that of PMMA (p=.005; Fig. 6b; Supplementary Fig. S6a). During the process of augmentation, voids in cancellous bone will be encapsulated and filled by dispersed bone cement. These cement-filled cancellous bones were identified as part of the cement dispersion volume via CT scan. Therefore, these results indicate that more cancellous bone will be encapsulated during dispersion when using the same volume of CPN as PMMA. Similar results were obtained when comparing dispersion ratios. The CPN dispersion ratio was significantly higher than the PMMA dispersion ratio (p=.001; Supplementary Fig. S6b). Moreover, CPN had better dispersion characteristics as evidenced by the results of the contrast VP augmentation experiment. The dispersion volume of CPN was significantly greater than that of PMMA when comparing the two sides of the three L5 vertebrae (p=.033; Fig. 6c; Supplementary Fig. S7a). Likewise, in all three L5 vertebrae, the dispersion ratio of CPN was significantly higher than that of PMMA (p=.034; Supplementary Fig. S7b). More cancellous bones were encapsulated by CPN during the dispersion process, suggesting the formation of good interdigitation between CPN and bone tissue, which is beneficial for increasing the augmentation effect of CPN.

Bone cement dispersion in sheep vertebrae

The micro-CT analysis results for cement dispersion were consistent in the three planes. In the transverse plane, the ratio of cement cross-sectional area to injection volume was significantly higher with CPN than with PMMA (p=.001; Fig. 7b). The similar results were obtained for the ratios of cross-sectional area to injection volume in the coronal plane, suggesting that the dispersion of CPN was better than that of PMMA (p=.039; Fig. 7c). On sagittal plane, the ratio of CPN was also higher than PMMA in the sagittal plane, however the difference was not significant (p=.063; Fig. 7d).

Bone cement dispersion in open-cell rigid foam model

Micro-CT images of the open-cell rigid foam model indicated that CPN and PMMA have completely different dispersion modes. After injection, the PMMA cement presented as a contracted clump in the open-cell rigid foam model. However, the CPN cement block had many antennae extending outward, indicating that CPN was spreading to the surrounding area. As the L/S ratio decreased, the antennae-like protrusions of CPN cement block become more obvious (Fig. 8b). These protuberances increased the surface area of CPN in the foam. The calculated surface area results were consistent with results from the micro-CT image. The surface areas of CPN cement blocks with different L/S ratios were significantly greater than the surface area of PMMA cement (1,037±72 mm^2; (p<.05). The surface area of the 0.4 L/S ratio CPN was significantly greater than the surface areas of other L/S ratios (p<.05). There were no significant differences in surface areas among CPN groups with 0.6, 0.8, or 1.0 L/S ratio (p>.05; Fig. 8b).

Discussion

CPN and PMMA are two completely different types of bone cement. After mixing the cement powder with setting liquid, CPN has no drawing stage, and directly enters a doughing period. The curing of CPN begins with the doughing stage, in which CPN reveals viscoplasticity and high viscosity. Moreover, CPN does not generate heat during the curing and hardening process, thus avoiding the risk

of thermal damage to surrounding tissues. PMMA cement is liquid-like after mixing and has a drawing period of several minutes. The PMMA doughing period is very short, after which the PMMA rapidly solidifies. In addition, previous studies have proven that CPN, as a calcium phosphate cement-based cement, results in good osseo-integration [12] and that PMMA has no biological potential to integrate into bone since it is a nondegradable material [28]. These features make CPN a promising alternative to PMMA for vertebral augmentation surgery.

For clinical application in PKP, CPN cement must overcome the problem of low mechanical strength seen in many existing calcium phosphate-based cements [29], and more importantly, it must also avoid the complications caused by the use of PMMA, such as cement leakage and adjacent vertebral fracture [4,5,8]. Thus, circumventing cement leakage and mechanical augmentation are crucial for the application of CPN in PKP.

Bone cement leakage

Leakage of PMMA is a common clinical complication of PKP, which can cause serious damage in patients undergoing vertebral augmentation [4,5]. Therefore, the prevention of bone cement leakage is very important during vertebral augmentation surgery. Clinical PMMA cement is polymerized, in part, using a liquid monomer and is in a fluid-like sate after mixing; thus it is prone to leakage during injection. In PKP augmentation experiment on human cadaveric vertebra, anterior wall leakage occurred in the vertebrae augmented by PMMA or CPN (Table 2), which should be attributed to the severe ruptures of anterior wall when vertebral fracture models were created. Nevertheless, the incidence of anterior wall leakage in CPN group was still lower than that in PMMA (75% vs. 100%) and the average number of leakage sites per vertebra was less in the CPN group (Table 2). On contrary, the incidence of posterior wall leakage of CPN was 0, while posterior wall leakage occurred in 75% of the human vertebrae treated with PMMA (Table 2). Moreover, no leakage was found when using CPN for VP experiments (Fig. 1c, d; Table 2). These results clearly suggested that CPN have anti-leakage properties compared with PMMA. PMMA leakage during injection could be due to its inherent physiochemical property and is likely unavoidable when PMMA is used clinically. In the leakage test using the simulated leakage model, PMMA leaked along the channel in all tests, whether at the same injection speed or with the same injection force, while CPN was less affected by the channel and still dispersed uniformly (Fig. 2b, e). The anti-leakage characteristic of CPN was likely due to a difference in physiochemical property between CPN and PMMA. After mixing, CPN cement is in a semi-solid state through the hydration reaction and is less fluid than PMMA, thus it is more difficult for CPN to leak. Moreover, hydroxyl-rich starch in CPN cement likely interacts strongly with other inorganic particles via hydrogen bonds, which increases the viscosity of CPN [11]. High viscosity of bone cement had been proven to reduce leakage [30,21]. When the viscosity of PMMA was increased to the level of CPN, the leakage distance and volume of PMMA were still greater than CPN (Fig. 2b, c). These results suggest that properties of cement, other than just viscosity, may affect leakage. Starch is one of the important components of CPN. Starch not only increases the viscosity of CPN, but also makes CPN a viscoplastic cement with adhesiveness. Thus, CPN easily adhered to the surrounding porous structure and infiltrated it during injection. Therefore, the viscoplasticity of CPN may affect leakage, which, together with high viscosity, causes CPN to have a different leakage pattern compared to PMMA.

Bone cement augmentation

The high mechanical strength and stiffness of PMMA can lead to adjacent vertebral fractures when PMMA is used for vertebral augmentation [8]. Aged patients with secondary fractures face re-operation, which significantly increases medical costs and family burdens. CPN has moderate mechanical strength, which reduces the risk of adjacent vertebral fractures, making it a promising alternative to PMMA. Although the mechanical strength was lower for CPN compared to PMMA, both CPN and PMMA significantly enhanced the mechanical strength of cancellous bone (Fig. 4b). Furthermore, results of PKP experiments in human vertebrae and sheep vertebrae found that there was no significant difference in augmentation strength between CPN and PMMA even though augmentation strength was lower for CPN compared to PMMA (Fig. 3b, c). The mechanical compression test of the solid rigid foam model indicated that the augmentation effect of CPN was only slightly lower compared to PMMA (Fig. 5d). As far as long-term effects, CPN cement is a biodegradable filling material and will gradually degrade after injection, allowing new bone growth to eventually replace the cement [12] and leading to the regeneration of vertebral structure. However, PMMA is nondegradable and permanently remains in the vertebral body, thereby perpetuating the risk of adjacent vertebral fracture.

Bone cement dispersion

The dispersion volume of CPN was significantly greater than that of PMMA (Fig. 6b, c), indicating that significantly more bone tissue was wrapped by CPN during dispersion than by PMMA. One possible reason for the difference in dispersion volume is that CPN and PMMA have totally different dispersion modes. In micro-CT images of open-cell rigid foam, PMMA showed a curled mass, while CPN cement extended many antennae outward, demonstrating a trend for spreading to the surrounding area (Fig. 8b). Different dispersion modes might be attributed to the different viscosities and injection forces between CPN and PMMA during injection process. The unique dispersion characteristics of CPN not only increased the surface area of the bone

cement (Fig. 8b), but also facilitated penetration and encapsulation of the surrounding porous bone tissue. After the cement wrapped the porous cancellous bone, a strong interlocking effect appeared between the cement and bone, which is likely to significantly increase the augmentation strength of CPN. The results of PKP experiments in both cadaveric vertebrae and sheep vertebrae confirmed that CPN, with weak mechanical strength, produced an augmentation effect close to PMMA (Fig. 3b, c). During the dispersing process, the adhesiveness of CPN also might make CPN adhere to the surrounding cancellous bone, reducing the probability of leakage. Therefore, anti-leakage and dispersion properties of CPN were better compared to PMMA when viscosity, viscoplasticity, and adhesiveness were combined. Leakage decreased when the viscosity of PMMA was at the same level as CPN (Fig. 2c, d), though by this time, PMMA was at the end of the curing stage (Supplementary Fig. S2b, c) and its viscosity quickly increased. The rapid increase in viscosity prevented PMMA from dispersing into cancellous bone.

Another possible reason for the difference in dispersion volume of CPN and PMMA is that CPN is hydrophilic while PMMA is hydrophobic. When injected into the vertebral body, CPN might easily wet on the surface of three-dimensional porous structure of bone tissue and then spread into large areas. On the contrary, PMMA was probably difficult to wet on bone surface. In this case, CPN was more likely to encapsulate cancellous bone compared to PMMA, which may also result in differed dispersion characteristics.

This study was supported by funds from government. All the individuals involved in this study analyze and process the experimental results objectively without any bias.

Conclusions

CPN had augmentation strength close to that of PMMA when used for PKP in cadaveric vertebrae, sheep vertebrae, and solid rigid foam models. To the best of our knowledge, this is the first time that imaging analysis showed that CPN has a completely different dispersion pattern than PMMA. CPN diffused more easily into cancellous bone and encapsulated bone tissues in the dispersion process. The excellent dispersion of CPN created better interdigitation with cancellous bone, which enhanced the augmentation strength of CPN. Moreover, compared with PMMA, CPN showed anti-leakage properties in PKP application, which might also be related to its high viscosity and viscoplasticity.

Acknowledgments

This study has been funded by National Natural Science Foundation of China (Nos. 81622032 and 51672184), Principal Project of Natural Science Research of Jiangsu Higher Education Institutions (No. 17KJA180011), and Jiangsu Innovation and Entrepreneurship Program. No benefits in any form have been or will be received from a commercial party related directly or indirectly to the subject of this article.

Supplementary materials

Supplementary material associated with this article can be found in the online version at https://doi.org/10.1016/j.spinee.2019.06.007.

Reference

[1] Kendler DL, Bauer DC, Davison KS, Dian L, Hanley DA, Harris ST, et al. Vertebral fractures: clinical importance and management. Am J Med 2016;129. 221.e1-221.e10.
[2] Lange A, Zeidler J, Braun S. One-year disease-related health care costs of incident vertebral fractures in osteoporotic patients. Osteoporos Int 2014;25:2435–43.
[3] Zhao G, Liu X, Li F. Balloon kyphoplasty versus percutaneous vertebroplasty for treatment of osteoporotic vertebral compression fractures (OVCFs). Osteoporos Int 2016;27:2823–34.
[4] Xiang GH, Tong MJ, Lou C, Zhu SP, Guo WJ, Ke CR. The role of unilateral balloon kyphoplasty for the treatment of patients with OVCFS: a systematic review and meta-analysis. Pain Physician 2018;21:91–110.
[5] Wang H, Sribastav SS, Ye F, Yang C, Wang J, Liu H, et al. Comparison of percutaneous vertebroplasty and balloon kyphoplasty for the treatment of single level vertebral compression fractures: a meta-analysis of the literature. Pain Physician 2015;18:209.
[6] Belkoff SM, Molloy S. Temperature measurement during polymerization of polymethylmethacrylate cement used for vertebroplasty. Spine 2003;28:1555–9.
[7] Jmf I, Khd I. Pulmonary embolism from cement augmentation of the vertebral body. Asian Spine J 2018;12:380–7.
[8] Lin D, Hao AJ, Li L, Wang L, Zhang H, Zou W, et al. Effect of bone cement volume fraction on adjacent vertebral fractures after unilateral percutaneous Kyphoplasty. Clin Spine Surg 2017;30:E270–5.
[9] Gao C, Liu H, Yang H, Yang L. Fabrication and characterization of injectable calcium phosphate-based cements for Kyphoplasty. Mater Technol 2016;30(sup8):B256–63.
[10] Liu H, Liu B, Gao C, Meng B, Yang AH, Yu H, et al. Injectable, biomechanically robust, biodegradable and osseointegrative bone cement for percutaneous kyphoplasty and vertebroplasty. Int Orthop 2017;42:125–32.
[11] Liu H, Guan Y, Wei D, Gao C, Yang H, Yang L. Reinforcement of injectable calcium phosphate cement by gelatinized starches. J Biomed Mater Res B Appl Biomater 2016;104:615–25.
[12] Sun H, Liu C, Liu H, Bai Y, Zhang Z, Li X, et al. A novel injectable calcium phosphate-based nanocomposite for the augmentation of cannulated pedicle-screw fixation. Int J Nanomed 2017;12:3395–406.
[13] Liu C, Liu HL, Sun HL, Yang HL, Li CD, Yang L. Development and optimization of biodegradable calcium phosphate-based nanocomposite for the application of spinal fixation. Ferroelectrics 2018;527:162–9.
[14] Kanis JA. Assessment of fracture risk and its application to screening for postmenopausal osteoporosis: synopsis of a WHO report. WHO Study Group. Osteoporos Int 1994;4:368–81.
[15] Chen LH, Tai CI, Lee DM, Lai PL, Lee YC, Niu CC, et al. Pullout strength of pedicle screws with cement augmentation in severe osteoporosis: a comparative study between cannulated screws with cement injection and solid screws with cement pre-filling. BMC Musculoskelet Disord 2011;12. 33-33.
[16] Tan E, Wang T, Pelletier MH, Walsh WR. Effects of cement augmentation on the mechanical stability of multilevel spine after vertebral compression fracture. J Spine Surg 2016;2:111–21.
[17] Kallemeier PM, Beaubien BP, Buttermann GR, Polga DJ, Wood KB. In vitro analysis of anterior and posterior fixation in an experimental unstable burst fracture model. J Spinal Disord Tech 2008;21:216–24.
[18] Zheng Z, Luk KD, Kuang G, Li Z, Lin J, Lam WM, et al. Vertebral augmentation with a novel Vessel-X bone void filling container system and bioactive bone cement. Spine 2007;32:2076–82.

[19] Perry A, Mahar A, Massie J, Arrieta N, Garfin S, Kim C. Biomechanical evaluation of kyphoplasty with calcium sulfate cement in a cadaveric osteoporotic vertebral compression fracture model. Spine J 2005;5:489–93.
[20] Bohner M, Gasser B, Baroud G, Heini P. Theoretical and experimental model to describe the injection of a polymethylmethacrylate cement into a porous structure. Biomaterials 2003;24:2721–30.
[21] Baroud G, Crookshank M, Bohner M. High-viscosity cement significantly enhances uniformity of cement filling in vertebroplasty: an experimental model and study on cement leakage. Spine 2006;31:2562–8.
[22] Molloy S, Mathis JM, Belkoff SM. The effect of vertebral body percentage fill on mechanical behavior during percutaneous vertebroplasty. Spine 2003;28:1549–54.
[23] Lewis G, Towler MR, Boyd D, German MJ, Wren AW, Clarkin OM, et al. Evaluation of two novel aluminum-free, zinc-based glass polyalkenoate cements as alternatives to PMMA bone cement for use in vertebroplasty and balloon kyphoplasty. J Mater Sci Mater Med 2010;21:59–66.
[24] Johnson AE, Keller TS. Mechanical properties of open-cell foam synthetic thoracic vertebrae. J Mater Sci Mater Med 2008;19:1317–23.
[25] Keller TS, Nathan M. Height change caused by creep in intervertebral discs: a sagittal plane model. J Spinal Disord 1999;12:313–24.
[26] Panjabi MM, Takata K, Goel V, Federico D, Oxland T, Duranceau J, et al. Thoracic human vertebrae. Quantitative three-dimensional anatomy. Spine 1991;16:888–901.
[27] Magerl F, Aebi M, Gertzbein SD, Harms J, Nazarian S. A comprehensive classification of thoracic and lumbar injuries. Eur Spine J 1994;3:184–201.
[28] Lieberman IH, Togawa D, Kayanja MM. Vertebroplasty and kyphoplasty: filler materials. Spine J 2005;5(6 Suppl):305S–16S.
[29] Zhang J, Liu W, Schnitzler V, Tancret F, Bouler JM. Calcium phosphate cements for bone substitution: chemistry, handling and mechanical properties. Acta Biomaterialia 2014;10:1035–49.
[30] Xin L, Bungartz M, Maenz S, Horbert V, Hennig M, Illerhaus B, et al. Decreased extrusion of calcium phosphate cement versus high viscosity PMMA cement into spongious bone marrow—an ex vivo and in vivo study in sheep vertebrae. Spine J 2016;16:1468–77.